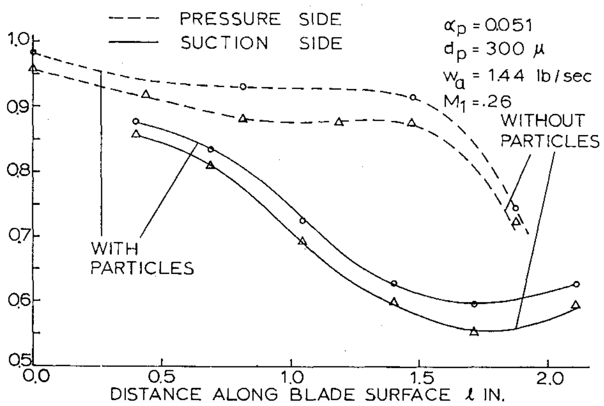

Fig. 7 Nondimensional pressure distribution on blade.

Test Results and Discussion

The experimental data show that the pressure distribution on the blade suction and pressure sides is affected by the presence of solid particles. Figures 4 and 5 show the pressure distribution on the blade for the cases with and without particles. These two figures represent a constant mean particle diameter $d_p = 50\ \mu$ and for a constant particle concentration α. The air mass flows are $W_a = 0.771$ and 1.45 lb/sec, correspondingly.

It can be observed that the pressure distributions for flows with particles are increased by a small amount with respect to those corresponding to the particle free case. A comparison of Figs. 4 and 5 indicates that the nondimensional pressure distribution over the blades will rise with a corresponding increase in Mach number or mass flow rate. This effect is intensified as the Mach number increases. This is a consequence of the rise in the level of turbulence, hence, an increase in pressure. Figures 6 and 7 show the same general trend for the case of $d_p = 300\ \mu$.

The pressure difference between flows with and without particles remains nearly constant despite the decrease in the concentration factor α and rise in the Mach number. It may be concluded from these observations that the deviation in pressure distribution is larger for a higher level of the concentration α. This increase in α will result in a drop in gas momentum and more particle collisions. This is made apparent by a rise in the pressure distribution.

The effect of a change in the particle material density $\bar{\rho}_p$ for different particle diameters d_p is difficult to assess. The reason for this is that it is necessary to use either the same particle material but different diameters, or vice versa. These requirements are difficult to meet because of the lack of a commercial source for such particles. However, in order to have some idea of the effect of changing d_p and $\bar{\rho}_p$, a comparison can be made between Figs. 5 and 7. These data are for the same concentration factor α, but with a sixfold increase in d_p from 50 to 300 μ accompanied by a one-third drop in $\bar{\rho}_p$ from 1.60 to 0.64 g/cm³. It will be observed that there is a slightly higher pressure rise in Fig. 7. This results from the increased particle inertia because of the larger particle diameters.

Conclusion

The measurements show that the particle sizes and concentrations change the pressure distribution along the cascades and, consequently, effect the basic performance of the turbine or compressor.

Reference

[1] Tabakoff, W. and Hussein, M., "An Experimental Study of the Effect of Solid Particles on the Pressure at Blade Surface in Cascade," Project Themis Rept. 70-8, University of Cincinnati, Cincinnati, Ohio, March 1970; also U.S. Government Research and Development Rept. AD-703896.

A Correction for Compressible Subsonic Planar Flow

HELGE NØRSTRUD*
Lockheed-Georgia Company, Marietta, Ga.

THE Prandtl-Glauert similarity rule describes the pressure distribution on an airfoil in a compressible uniform stream of Mach number M_∞ in terms of the incompressible pressure distribution by the well-known formula

$$c_{pM_\infty} = c_{pi}/(1 - M_\infty^2)^{1/2} \qquad (1)$$

where $c_{pi} = c_{pM_\infty=0}$ designates the incompressible pressure coefficient. This simple compressibility correction rule has been extensively applied in aerodynamics and is of fundamental importance in linearized flow analysis. However, its limitations for freestream Mach numbers approaching unity are evident from Eq. (1). Another deficiency in adopting the Prandtl-Glauert correction formula for high subsonic speeds is because of its one dimensionality, which again precludes a correct prediction of the pressure distribution at these speeds. The present Note is concerned with an improvement over the Prandtl-Glauert rule in the latter sense. A compressibility correction formula will be given which is essentially a relationship between local variables, but which can be understood as being able to include some global effects.

The earliest improvements to the Prandtl-Glauert compressibility rule came as a natural extension from the hodograph theory of compressible flow. The Kármán-Tsien formula[1] and the works of Ringleb[2] and Temple and Yarwood[3] are examples of this development. Garrick and Kaplan[4] subsequently gave a unified analysis of previous results and also introduced some new relations. Krahn[5] arrives at his formula by writing the incompressible velocity as the geometric mean of the compressible velocity and the stream density. This procedure, however, leads to an implicit expression for the compressible pressure coefficient. The relation given by

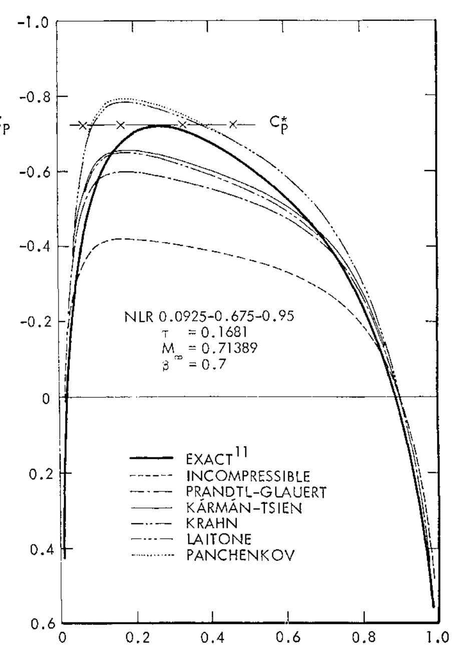

Fig. 1 Chordwise pressure distribution as obtained from various compressibility correction formulas.

Received August 17, 1970.

* Scientist, Aerospace Sciences Laboratory. Member AIAA.

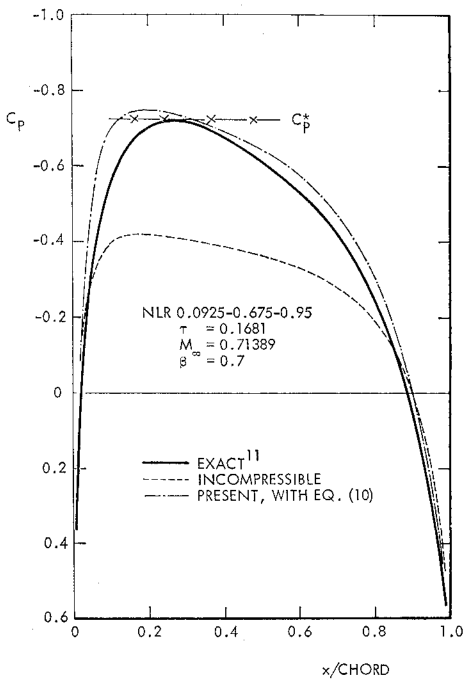

Fig. 2 Chordwise pressure distribution as given by the present analysis.

Laitone[6] does not have this drawback and is obtained by using the local Mach number M rather than M_∞ in Eq. (1). A second-order compressibility rule is due to Van Dyke,[7] but is only applicable to a particular class of airfoils as pointed out by Imai.[8] Finally, the recent work of Panchenkov[9] should be mentioned in which a pressure correction formula is obtained from the transonic small disturbance equation.

The present analysis is also based on this nonlinear partial differential equation which can be expressed as

$$\frac{\partial u}{\partial x} + \frac{1}{1 - M_\infty^2}\frac{\partial v}{\partial y} = \frac{1}{1/M_\infty^* - 1}\left(\frac{u - u_\infty}{u_\infty}\right)\frac{\partial u}{\partial x} \tag{2}$$

Here the velocity components u,v are defined in a Cartesian coordinate system x,y where x designates the direction of the undisturbed flow. The flow is assumed inviscid and isentropic, and Eq. (2) must be supplemented by the condition of irrotationality

$$(\partial u/\partial y) - (\partial v/\partial x) = 0 \tag{3}$$

Now the integral equation approach of transonic flow will be adopted to rewrite Eq. (2) to yield the integral formulation

$$\frac{1}{2(1/M_\infty^* - 1)}\left(\frac{u - u_\infty}{u_\infty}\right)^2 - \left(\frac{u - u_\infty}{u_\infty}\right) + \frac{1}{\beta}\left(\frac{u_i - u_\infty}{u_\infty}\right) = \frac{1}{4\pi(1/M_\infty^* - 1)}\iint_{-\infty}^{\infty}\left(\frac{u - u_\infty}{u_\infty}\right)^2 \times \frac{(x - \xi)^2 - \eta^2}{[(x - \xi)^2 + \eta^2]^2}\,d\xi d\eta \tag{4}$$

Here $\beta = (1 - M_\infty^2)^{1/2}$ is the Prandtl-factor and the subscript i designates the incompressible solution to the particular airfoil problem. It will be further assumed that the perturbation velocity in the integrand of Eq. (4) decays perpendicular to the x axis according to the law (written for the upper half plane $\beta y \geqslant 0$):

$$\frac{u(x,+\beta y) - u_\infty}{u_\infty} = \frac{u(x,+0) - u_\infty}{u_\infty}\left[1 - \frac{\beta y}{r}\right]$$
$$0 \leqslant \beta y \leqslant r, r < \beta y < \infty = 0 \tag{5}$$

This implies that the perturbation velocity reduces linearly from its maximum value at the profile boundary (taken as the x axis) to zero at and beyond a distance $y = r/\beta$. The parameter $r = r(x)$ shall be defined with the aid of Eq. (3) as

$$r(x) = \left|\frac{1}{g''(x)}\left(\frac{u_i(x) - u_\infty}{u_\infty}\right)\right| \tag{6}$$

where $g(x)$ designates the thickness distribution of the airfoil.

After substituting Eq. (5) in the double integral of Eq. (4), an integration can be performed in the y direction. If one, in addition, approximates the quadratic terms of the perturbation velocity with the corresponding Prandtl-Glauert value, one obtains for the perturbation velocities on the x axis the following expression:

$$\frac{u(x) - u_\infty}{u_\infty} = \frac{1}{\beta}\left(\frac{u_i(x) - u_\infty}{u_\infty}\right) + \frac{1}{2(1 - M_\infty^2)(1/M_\infty^* - 1)}\left[\left(\frac{u_i(x) - u_\infty}{u_\infty}\right)^2 - \int_{\xi=-\infty}^{\infty}\left(\frac{u_i(\xi) - u_\infty}{u_\infty}\right)^2 E(|x - \xi|;r)d\xi\right] \tag{7}$$

The influence function $E = E(|x - \xi|;r)$ is evaluated[10] as

$$E(z) = E\left(\frac{|\xi - x|}{r}\right) = \frac{2}{\pi r}\left\{\frac{1}{2}\ln(1 + z^{-2}) + z\arctan z^{-1} - 1\right\}$$

The single integral in Eq. (7) can now for a given incompressible velocity distribution be integrated (analytical or numerical) to yield the compressible solution. The associated pressure coefficient is then calculated by using the isentropic relation

$$c_p(x) = \frac{2}{\varkappa M_\infty^2}\left\{\left[1 + \frac{1}{2}(\varkappa - 1)M_\infty^2 \times \left(1 - \frac{u^2(x)}{u_\infty^2}\right)\right]^{\varkappa(\varkappa-1)} - 1\right\} \tag{8}$$

where $\varkappa$ designates the ratio of specific heats. However, in order to express the compressible velocity distribution in terms involving only correction factors to the incompressible solution, it is necessary to seek an approximate formulation for the latter distribution. The simplest way to achieve this is to represent the chordwise ($0 \leqslant x \leqslant 1$) distribution at each location with a uniform value equal to the particular local value.

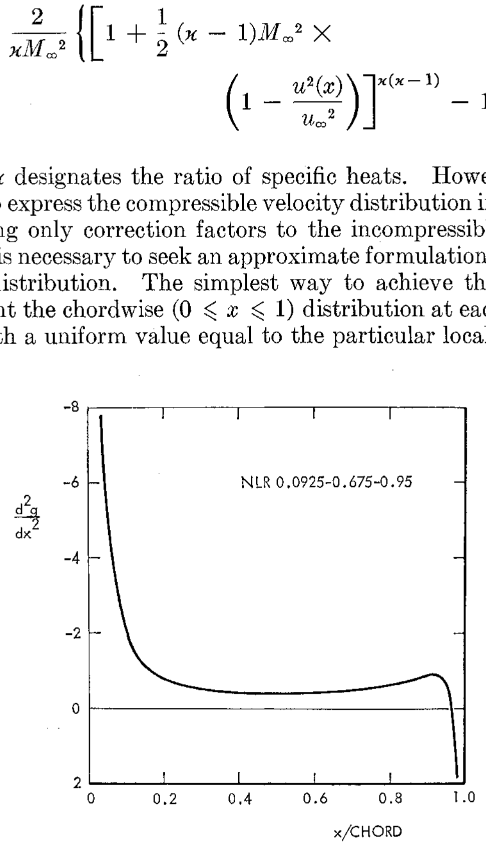

Fig. 3 Chordwise distribution of profile curvature.

The integral in Eq. (7) will then read

$$\left[\frac{u_i(x) - u_\infty}{u_\infty}\right]^2 \int_{\xi=0}^{1} E(|x - \xi|;r)d\xi = \frac{1}{\pi}\left(\frac{u_i(x) - u_\infty}{u_\infty}\right)^2 \left\{r^{-1}\ln(1 + r^2) + 2\arctan r^{-1} + (1 + r^{-2})\arctan r - r^{-1} - \frac{\pi}{2}\right\}$$

or be written in a series form,

$$\left[\frac{u_i(x) - u_\infty}{u_\infty}\right]^2 \int_{\xi=0}^{1} E(|x - \xi|;r)d\xi = \frac{1}{\pi}\left(\frac{u_i(x) - u_\infty}{u_\infty}\right)^2 \left\{\frac{\pi}{2} - \frac{1}{3}r + \frac{1}{30}r^3 - \ldots\right\} \quad (r < 1) \qquad (9)$$

Equation (9), with the first two terms retained in the series expansion, is substituted back in Eq. (7) and one obtains the desired result,

$$\frac{u(x) - u_\infty}{u_\infty} = \frac{1}{\beta}\left[\frac{u_i(x) - u_\infty}{u_\infty}\right] + \frac{3\pi + 2r}{12\pi(1 - M_\infty{}^2)(1/M_\infty{}^* - 1)}\left[\frac{u_i(x) - u_\infty}{u_\infty}\right]^2 \qquad (10)$$

Here $r = r(x)$ is determined from Eq. (6) and the value for the pressure coefficient c_p can again be found from Eq. (8).

The compressibility rule described by Eq. (10) will be tested on a symmetrical blunt-nosed airfoil. The exact pressure distribution for this airfoil at nearly critical freestream Mach number is given in Ref. 11 together with geometric profile data. These again have been utilized to calculate the incompressible solution by using a mapping method which is briefly described in Ref. 12. Various compressibility corrections were applied to the incompressible values, and the obtained results are plotted together with the exact values in Fig. 1. It can be seen that none of the applied correction formulas can satisfactorily account for the global change of the pressure distribution with increasing freestream Mach number. This is not surprising since the correction factors are constants based on the freestream condition only. For a discussion of introducing the profile surface slope into the correction factors, the reader is referred to the work of Wilby.[13]

In Fig. 2 the result of the present analysis as applied to the same airfoil problem of Fig. 1 is given. Due to the additional dependence on profile curvature (see Fig. 3), the compressibility correction defined by Eq. (10) yields reduced corrections to the Prandtl-Glauert value at locations of large curvature, e.g., at the nose region. This is the essential feature of the present approach and it is viewed as an improvement over other correction methods.

References

[1] Tsien, H., "Two-Dimensional Subsonic Flow of Compressible Fluids," *Journal of the Aeronautical Sciences*, Vol. 6, No. 10, Aug. 1939, pp. 399–407.

[2] Ringleb, F., "Näherungsweise Bestimmung der Druckverteilung einer adiabatischen Gasströmung," FB 1284, 1940, Zentrale für wissenschaftliches Berichtswesen der Luftfahrtforschung des Generalluftzeugmeisters (ZWB), Berlin.

[3] Temple, G. and Yarwood, J., "The Approximate Solution of the Hodograph Equations for Compressible Flow," Rept. S.M.E. 3201, June 1942, British Royal Aircraft Establishment, Farnborough, England.

[4] Garrick, I. E. and Kaplan, C., "On the flow of a compressible fluid by the hodograph method. I—Unification and extension of present-day results," Rept. 789, Jan. 1944, NACA.

[5] Krahn, E., "Näherungsverfahren zur Berechnung kompressibler Unterschallströmung," *Zeitschrift für Angewandte Mathematik und Mechanik*, Band 29, Heft 1/2, Jan./Feb. 1949, pp. 2–3.

[6] Laitone, E. V., "New Compressibility Correction for Two-Dimensional Subsonic Flow," *Journal of the Aeronautical Sciences*, Vol. 18, No. 5, May 1951, p. 350.

[7] Van Dyke, M. D., "The Second-Order Compressibility Rule for Airfoils," *Journal of the Aeronautical Sciences*, Vol. 21, No. 9, Sept. 1954, pp. 647–648.

[8] Imai, I., "The Second-Order Thin Airfoil Theory for Compressible Flow," *Journal of the Aeronautical Sciences*, Vol. 22, No. 4, April 1955, pp. 270–271.

[9] Panchenkov, A. N., "Nesushchaya Poverkhnost' v Okolozvukovom Potoke Gaza," edited by I. L. Rozovskii, Gidrodinamika Bolshikh Skorostei, Izdatelstvo Naukova Dumka, Kiev, 1967, pp. 7–20 (English translation available from SLA as 68-12561-01A).

[10] Nörstrud, H., "Numerische Lösungen von schallnahen Strömungen um ebene Profile," Ph.D. thesis, June 1968, Vienna Institute of Technology, Austria.

[11] Boerstoel, J. W., "Symmetrical subsonic potential flows around quasi-elliptical aerofoil sections," NRL TR 68016, 1968, National Aerospace Laboratory, Amsterdam, Holland.

[12] Asaka, S. and Hayasi, N., "An improved thin-airfoil theory for an arbitrary airfoil in a subsonic flow," ER-8979, March 1969, Lockheed-Georgia Research, Marietta, Ga.

[13] Wilby, P. G., "The Calculation of Sub-Critical Pressure Distributions on Symmetric Aerofoils at Zero Incidence," NPL Aero Rept. 1208, March 1967, National Physical Laboratory, Teddington, England.

Rapid Calculation of Inviscid and Viscous Flow over Arbitrary Shaped Bodies

H. A. Dwyer,* E. D. Doss,† and A. Goldman†
University of California, Davis, Calif.

Introduction

THE purpose of this Note is to show how the high Reynolds number viscous and inviscid flow over arbitrary shaped two-dimensional bodies, and in particular airfoils, can be calculated very rapidly and exactly with a modern digital computer. The calculations will only be carried out for the high Reynolds number case, so that the boundary layer and potential flow approximations can be made. (This of course, restricts the viscous flow calculation to a region of flow in front of the separation point.) Also, the results presented in this paper will be limited to incompressible flow and laminar flow in the boundary layer; although turbulent flow calculations have been carried out.

The basic methods which are employed in the paper are the following: 1) a numerical solution of the potential flow equations by a general method developed by Theodorsen and Garrick,[1] and 2) finite difference solution[2,3] of the boundary-layer equations near the body surface up to the point of flow separation. These two methods were combined into one computer program which calculated the potential and boundary-layer flow over the body in a matter of seconds on the digital computer. The input for this program consisted solely of the body coordinates, angle of attack or net circulation, and the fluid properties. (For the purpose of illustration the calculation technique was applied to the flow over a NACA 0012 airfoil section.)

One of the main reasons for writing this Note is to point out the power of the digital computer in solving these types of difficult flow problems. As will be shown in the following, the methods used are more exact and less time consuming than all of the approximate techniques still employed in design and

Received July 22, 1970.

* Associate Professor, Mechanical Engineering Department. Member AIAA.

† Research Assistant.